

## Extremely low threshold current density strained InGaAs/ AlGaAs quantum well lasers by molecular beam epitaxy

Yang Guowen, Xu Junying, Xiao Jianwei, Xu Zuntu,  
Zhang Jingming, Zheng Wanhua, Zeng Yiping and Chen Lianghui

(Institute of Semiconductors, The Chinese Academy of Sciences,  
National Integrated Optoelectronics Lab., Beijing 100083)

**Abstract** Using solid source molecular beam epitaxy we have fabricated strained InGaAs/AlGaAs graded index separate confinement single quantum well lasers emitting at 0.98  $\mu\text{m}$ . For broad-area, uncoated Fabry-Perot devices with cavity lengths of 560 $\mu\text{m}$ , the threshold current density is 145A/cm<sup>2</sup>, a value which is believed to be the lowest value ever reported domestically for quantum well laser diodes in any materials system. The external differential quantum efficiency is 35% per facet.

**PACC:** 4255P, 4280R, 7360F

### 1. Introduction

The InGaAs/AlGaAs strained quantum well lasers emitting at  $\sim 1\mu\text{m}$  have many desirable features, due to the changes of energy band structure induced by strained nature of the active region. (1) the extended wavelength capability for long wavelength lasers ( $0.9 \leq \lambda \leq 1.1\mu\text{m}$ )<sup>[1]</sup>, and these wavelength range cannot be achieved with lattice-matched materials such as GaAs/AlGaAs system (0.7—0.9 $\mu\text{m}$ ) and InP/InGaAsP system (1.1—1.65 $\mu\text{m}$ ), (2) lower threshold current density ( $J_{\text{th}}$ )<sup>[2]</sup>, (3) higher temperature operation due to reduced Auger recombination<sup>[3]</sup>, (4) high modulation frequency due to larger gain coefficient<sup>[2]</sup>, (5) high output powers due to more than several factors higher facet catastrophic optical damage (COD) limit compared with that of GaAs and AlGaAs materials<sup>[2]</sup>, (6) high efficiency and low noise pumping sources for Er<sup>3+</sup>-doped fiber amplifiers at 0.98 $\mu\text{m}$ <sup>[4]</sup>, (7) obtaining visible blue-green laser emission by frequency doubling, (8) long life operation reported in recent years<sup>[5]</sup>, *et al.* and just because of these above advantages, it has recently stimulated much interest, the lowest threshold current density has been decreased to less than 100A/cm<sup>2</sup> reported by now<sup>[6]</sup>. There is still quite a gap compared to that of abroad. In this paper we reported the new results obtained in our laboratory.

### 2. Laser design and material growth

The growth of the laser material was performed in a RIBER MBE 32P system

on Si-doped ( $n^+$ ,  $10^{18}\text{cm}^{-3}$ )  $4^\circ$ -off (100) towards  $\langle 111 \rangle$  A GaAs substrates. Before being loaded into the growth chamber, each wafer was prepared by the following processes: first degreased sequentially in trichloroethylene, acetone, and methanol for three times, etched in  $5\text{H}_2\text{SO}_4:1\text{H}_2\text{O}_2:1\text{H}_2\text{O}$  solution for several minutes, then rinsed in  $18\text{M}\Omega\text{cm}$  running de-ionized water and finally blown dry with filtered nitrogen gas. The cleaned substrates were then mounted onto a molybdenum block with high purity indium and transferred into the preparation chamber immediately. After degassing at  $400^\circ\text{C}$  for about one hour, the substrate was placed into the growth chamber, followed by the usual deoxide process at temperature  $580^\circ\text{C}$ , for good uniformity, the wafer holder was rotated continuously with  $20\text{rpm}$  during MBE growth.

The laser design is a graded-index (GRIN) separately confinement single quantum well structure, as illustrated in Fig.1. It consists of a  $0.7\mu\text{m}$ -thick  $n^+$ -GaAs ( $2 \times 10^{18}\text{cm}^{-3}$ ) buffer layer, a  $0.15\mu\text{m}$   $n^+$ - $\text{Al}_x\text{Ga}_{1-x}\text{As}$  ( $1 \times 10^{18}\text{cm}^{-3}$ ) compositionally graded layer ( $x$  value from 0.2 to 0.6), a  $1.2\mu\text{m}$   $n$ - $\text{Al}_{0.6}\text{Ga}_{0.4}\text{As}$  ( $1 \times 10^{18}\text{cm}^{-3}$ ) cladding layer, a  $0.2\mu\text{m}$  undoped linearly graded index  $\text{Al}_x\text{Ga}_{1-x}\text{As}$  ( $x$  from 0.6 to 0.2) waveguide layer, a  $40\text{\AA}$  undoped  $\text{In}_{0.3}\text{Ga}_{0.7}\text{As}$  strained active layer surrounded on both sides by a  $100\text{\AA}$ -thick undoped GaAs spacer layer, a  $0.2\mu\text{m}$  undoped  $\text{Al}_x\text{Ga}_{1-x}\text{As}$  ( $x$  from 0.2 to 0.6) graded waveguide layer, a  $1.2\mu\text{m}$   $p$ - $\text{Al}_{0.6}\text{Ga}_{0.4}\text{As}$  ( $1 \times 10^{18}\text{cm}^{-3}$ ) upper cladding layer, and finally a  $0.2\mu\text{m}$   $p$ -GaAs ( $1 \times 10^{19}\text{cm}^{-3}$ ) top layer and a  $200\text{\AA}$  ohmic contact layer ( $5 \times 10^{19}\text{cm}^{-3}$ ). The  $n$  and  $p$  dopants were Si and Be, respectively.

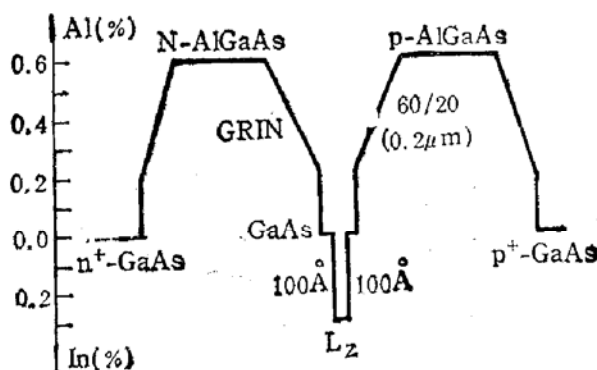


Fig. 1 Schematic diagram of the strained InGaAs/AlGaAs graded index (GRIN) separate confinement heterostructure (SCH) single quantum well (SQW) laser

During the MBE growth, all the AlGaAs layers including  $n$ -,  $p$ - cladding layers, compositionally graded layers and 80% of the graded waveguide layers, were grown at constant temperature of  $700^\circ\text{C}$ , the GaAs and InGaAs quantum well region were grown at  $560^\circ\text{C}$ . The growth temperature was ramped from  $700^\circ\text{C}$  to  $560^\circ\text{C}$  or vice-versa during the remaining 20% of GRIN layer adjacent to the quantum well region. The GaAs buffer and upper  $p$ -GaAs layer were grown at  $600^\circ\text{C}$ . No growth interruption was used during the growth. V/III flux ratio was selected near-critical arsenic-stabilized condition.

Because of the higher compressive strain induced by the larger InAs content of 0.3 used in the active layer, when the active layer thickness was thinner than the critical thickness, the threshold current density will decrease compared with that of

InAs content of 0.2<sup>[7]</sup>. In order to adjust the emission wavelength at 0.98 $\mu\text{m}$ , the quantum well thickness was chosen to be about 40 Å.

### 3. Device Fabrication and Characteristics

After MBE growth, a 1000  $\times$  Nomarski phase contrast microscopy or scanning electron microscopy was used to examine the surface. Except some occasionally observed oval defects, featureless surface morphologies were obtained.

A conformal 2000 Å-thick  $\text{SiO}_2$  was deposited over the entire p-surface by Plasma-Enhanced Chemical Vapor Deposition (PECVD), then contact stripes were opened by standard photolithograph. After the process of thinning, deposition of electrode film (TiPtAu as p-contact and AuGeNi as n-contact), cleaving, testing and soldering (p side down), the broad-area quantum well laser diodes were obtained.

Light output power measurement as a function of injected current was performed for each laser. The measured values of threshold current and slope efficiency were very close, which indicates very good uniformity. A typical P-I curve was shown in Fig. 2, the cavity length, stripe width and threshold current were 560 $\mu\text{m}$ , 120 $\mu\text{m}$  and 97mA, respectively. From these data we can calculate that the broad-area  $J_{\text{th}}$  is 145A/ $\text{cm}^2$ , and this value takes no account of any current spreading, nor of the anti-guiding effects which widen the effective stripe width. If the cavity length was extended, the threshold current density will decrease further. From Fig. 2 we can see that the linear output power is more than 600mW, a power output of 0.5W per facet is achieved at an injected current approximately 1.28A. The external differential quantum efficiency ( $\eta_d$ ) of 35% per facet is obtained for the device.

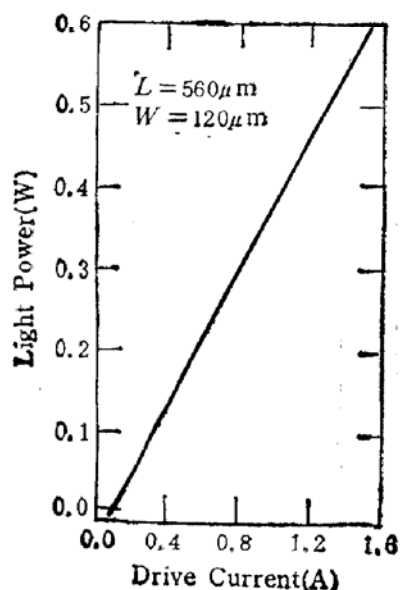


Fig. 2 Continuous wave light output as a function of drive current for a device of length 560 $\mu\text{m}$

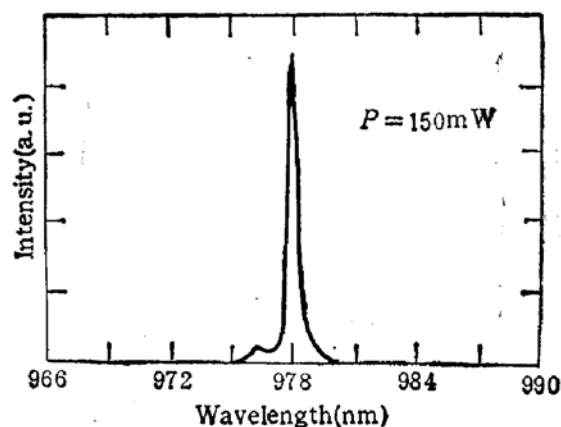


Fig. 3 Room temperature spectrum of strained InGaAs quantum well laser at 150mW. The peak wavelength is 978.1nm

We attribute this extremely low value of the threshold current density to the

following three factors: (1) the optimization of laser design, such as graded index waveguide layer and cladding regions with higher aluminum content which will produce larger optical confinement. (2) strained nature of the active layer produces the changes of energy band structure, namely, the removal of the heavy hole/light hole degeneracy, symmetrization of conduction and valence-band densities of states, and these make the population inversion more easier. (3) the high quality of the MBE-grown material, and this is also the very important factor. It results from optimizing separately each process condition, such as the substrate temperatures for both AlGaAs cladding and the InGaAs quantum well active layer, V/III flux ratio etc.

We know that the electron capture time is the shortest for single quantum well, and is monotonic function of well thickness.<sup>[6]</sup> When the thickness decreases, the carrier collection efficiency also decreases. The external quantum efficiency of the device was not high enough might be in some extent attributed to this reason.

The measured laser spectrum is shown in Fig.3, the emission wavelength is 978.1 nm under 150mW output power, and this wavelength will become longer at higher output power.

#### 4. Conclusion

By optimizing the laser structure and the process condition, we fabricated excellent uniformity and very low threshold current density strained InGaAs/AlGaAs quantum well diode lasers. The value of  $J_{th}$  decreases due to large optical confinement factor produced by high aluminum content cladding and linearly graded index waveguide layer. For higher performance operation, all the AlGaAs cladding layers should be grown at 700°C, so as to obtain high quality MBE growth material. Furthermore, the optimized growth temperature for InGaAs quantum well, and extremely clean growth environment are also key factors for high quality material growth.

#### Reference

- [1] D.J. Arent, K. Deneffe, C.VanHoof, J.De Boeck, and G. Borghs, *J. Appl. Phys.*, 1989, **66**:1739.
- [2] H. K. Choi and C. A. Wang, *Appl. Phys. Lett.*, 1990, **57**:321.
- [3] J. P. Van der Ziel and N. Chand, *Appl. Phys. Lett.*, 1991, **58**: 1437.
- [4] M. C. Wu, N. A. Olsson, D. Sivci, and A. Y. Cho, *Appl. Phys. Lett.*, 1990, **56**: 221.
- [5] S. L. Yellin, R. G. Waters, Y. C. Chen, B.A. Soltz, S.E. Fischer, D. Fekete, and J. M. Ballantyne, *Electron. Lett.*, 1990, **26**: 2083.
- [6] R. L. Williams, M. Dion, F.Chatenold, and K. Dzurko, *Appl. Phys. Lett.*, 1991, **58**(17):1816.
- [7] R. Ben-Michale, D. Fekete, and R. Sarfaty, *Appl. Phys. Lett.*, 1991, **59**:3219.
- [8] J. A. Brum and G. Bastard, *Phys. Rev.* 1986, **B33**: 1420.